

## Mechanism of the Formation of Donor States in Heat-Treated Silicon

W. KAISER, H. L. FRISCH, AND H. REISS  
*Bell Telephone Laboratories, Murray Hill, New Jersey*  
 (Received August 4, 1958)

A mechanism for the donor formation during heat treatment of silicon crystals is presented which accounts quantitatively for the complex kinetic phenomena and which is consistent with the known extra-kinetic information concerning this system. Atomically dissolved oxygen introduced during the growth of the silicon crystal reacts, in the course of heat treatment, to form a sequence of kinetically linked aggregates till finally a polymeric silica ( $\text{SiO}_2$ ) is formed. Only those aggregates which possess fewer than five bound oxygen atoms appear to act intensively as donors at room temperature, and in particular donor states produced around  $450^\circ\text{C}$  appear to consist principally of a donor  $[\text{SiO}_4]$  complex. The kinetic equations are integrated using a general-purpose analog computer for a variety of initial concentrations of oxygen, temperature, etc., and the results compare favorably with existing experimental observations.

### A. INTRODUCTION

IN recent years a considerable body of experimental literature has evolved concerning the "heat treatment" problem in silicon. As yet no theory of the phenomenon has been advanced capable of unifying all the diverse observations. In this paper we propose a model which appears capable of quantitatively correlating the kinetic data of heat treatment and which is consistent with the extra-kinetic information.

### B. PHENOMENA ASSOCIATED WITH THE HEAT TREATMENT OF SILICON

The salient facts are as follows:

(1) Fuller, Ditzenberger, Hannay, and Buehler<sup>1</sup> discovered a strong increase in donor concentration in silicon single crystals when the material was heated for periods of hours at  $460^\circ\text{C}$ . The general character of the donor formation is illustrated by Fig. 1 which shows donor concentration *versus* time of heat treatment at  $450^\circ\text{C}$ .<sup>2</sup> The concentration of donors reaches a characteristic maximum, which in this case is attained after about 70 hours, and subsequently decreases slowly. The logarithm of the difference—maximum donor concentration minus the donor concentration at a given time—plotted *versus* time gives a linear relationship for

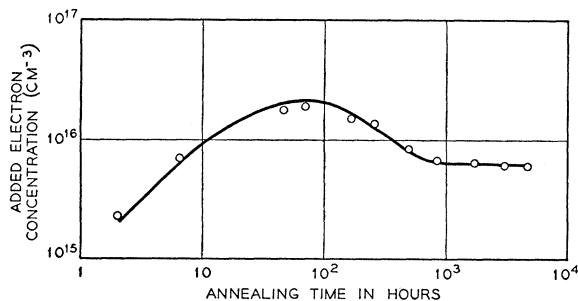


FIG. 1. Increase in electron concentration during annealing at  $450^\circ\text{C}$ . The curve is calculated from the extended model.

<sup>1</sup> Fuller, Ditzenberger, Hannay, and Buehler, *Phys. Rev.* **96**, 833 (1954) and *Acta Met.* **3**, 97 (1955).

<sup>2</sup> C. S. Fuller and R. A. Logan, *J. Appl. Phys.* **28**, 1427 (1957).

times prior to the appearance of the maximum (see Fig. 2).

(2) The same authors showed that the donor states, once formed in the specimen, can be removed rapidly by subsequent heating at temperatures above  $500^\circ\text{C}$ . Recently Fuller and Logan<sup>2</sup> gave further experimental

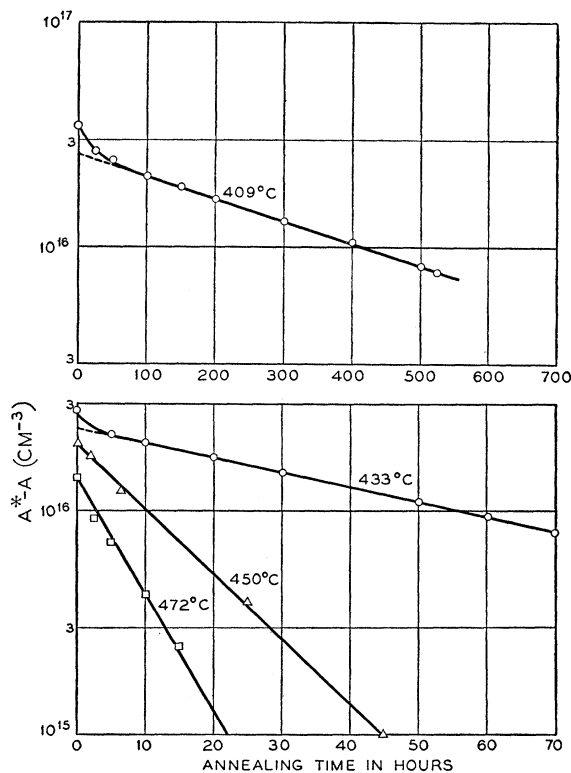


FIG. 2. The logarithm of the maximum donor concentration  $A^*$  minus the donor concentration  $A$  at time  $t$ , plotted *versus* time.

evidence for the subsequent disappearance of these donors at higher temperatures. Figure 9 of reference 2 illustrates the latter. The donor concentration appears to decay exponentially with time.

(3) Fuller and Logan<sup>2</sup> have also shown that at

temperatures below 450°C a considerably smaller rate of donor formation is observed and no maximum donor concentration is attained below about 430°C even upon heat treatment for periods of 500 hours. For samples prepared from the same crystal the time of attainment of the maximum (at temperatures where it is reached) appears to decrease with an increase in the temperature while the maximum donor concentration increases with decreasing temperature (Fig. 6). (See also Fig. 7 of reference 2.)

(4) Kaiser, Keck, and Lange<sup>3</sup> found oxygen as an impurity in a concentration of  $10^{18}$  atoms per  $\text{cm}^3$  in

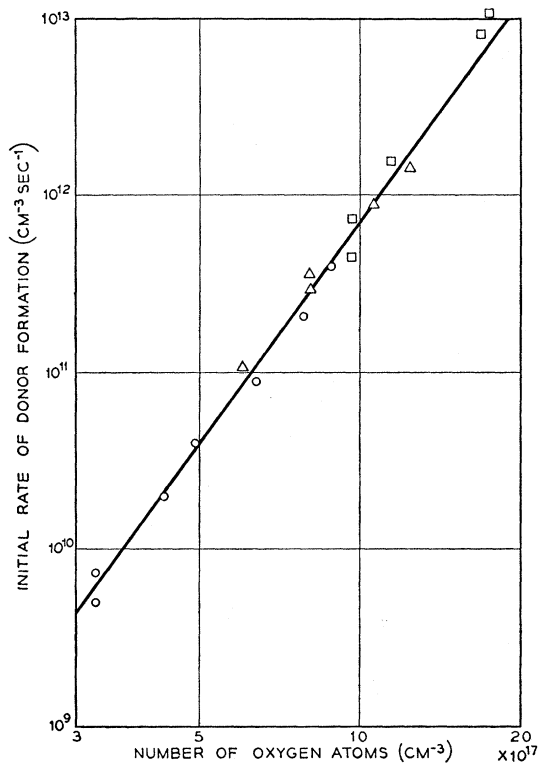


FIG. 3. Initial rate of donor formation *versus* the oxygen concentration after annealing at 450°C. Different symbols represent data obtained from different crystals.

silicon single crystals pulled from a melt contained in a quartz crucible. An infrared absorption band of silicon at  $9\ \mu$ <sup>4</sup> could be quantitatively correlated with the oxygen content of the crystal.<sup>5</sup> Combined electrical and optical investigations on silicon samples heat-treated at 450°C gave conclusive evidence that the formation of donor states depends upon the oxygen content.<sup>2,6,7</sup>

(5) The initial rate of donor formation is proportional to the fourth power of the oxygen concentration.<sup>6</sup>

<sup>3</sup> Kaiser, Keck, and Lange, *Phys. Rev.* **101**, 1264 (1956).

<sup>4</sup> H. J. Hrostowski and R. H. Kaiser, *Phys. Rev.* **107**, 966 (1957).

<sup>5</sup> W. Kaiser and P. H. Keck, *J. Appl. Phys.* **28**, 822 (1957).

<sup>6</sup> W. Kaiser, *Phys. Rev.* **105**, 1751 (1957).

<sup>7</sup> R. Logan, *J. Appl. Phys.* **28**, 819 (1957).

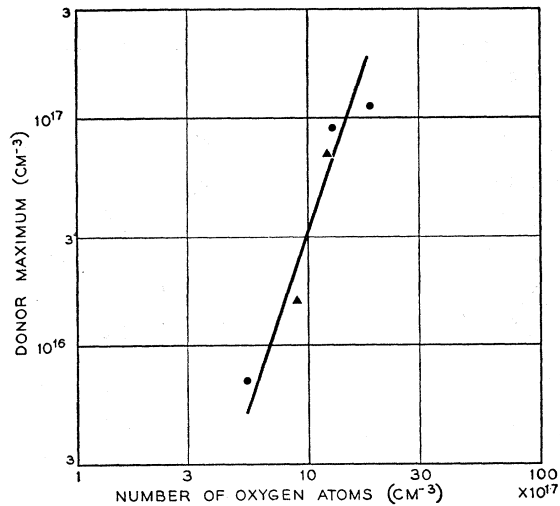


FIG. 4. Maximum donor concentration *versus* oxygen concentration after annealing at 450°C. ● specimen prepared in floating-zone equipment with oxygen in the ambient gas. ▲ pulled rotated crystals.

This fact is illustrated in Fig. 3 where data on a number of samples are plotted as the logarithm of the initial rate of donor formation *versus* the logarithm of the oxygen concentration.<sup>6</sup> The points are fitted by the line with a slope of four.

(6) It appears that the maximum donor concentration is approximately proportional to the third power of the oxygen concentration. This is seen from Fig. 4 where maximum donor concentration at 450°C is plotted *versus* the logarithm of the oxygen concentration of the crystal.<sup>8</sup>

(7) The time necessary to attain the maximum donor concentration at 450°C increases with decreasing oxygen concentration of the specimen.<sup>8</sup>

(8) In silicon crystals which are not rotated during the pulling process a considerably smaller number of donor states can be formed during heat treatment around 450°C.<sup>1</sup> These crystals are found to contain less oxygen than ingots pulled under similar conditions with rotation.<sup>4</sup>

(9) Silicon can dissolve oxygen up to a concentration of  $1.8 \times 10^{18}$  atoms per  $\text{cm}^3$  at its melting point.<sup>5,9</sup>

(10) The solid solubility for oxygen decreases with decreasing temperature (heat of solution  $\sim 1$  ev).<sup>10</sup> Therefore almost all pulled, rotated single crystals of silicon are supersaturated with oxygen over most of the temperatures.<sup>6</sup>

(11) Upon prolonged heating, aggregation of oxygen occurs in the specimen and the formation of  $\text{SiO}_2$  as a second phase is expected. At 1000°C the aggregate particles are large enough ( $\sim 0.1\ \mu$  in diameter) to give rise to Tyndall scattering effects.<sup>6</sup> Distinct optical

<sup>8</sup> R. A. Logan (to be published).

<sup>9</sup> W. Kaiser and J. Breslin, *J. Appl. Phys.* **29**, 1292 (1958).

<sup>10</sup> H. J. Hrostowski and R. H. Kaiser, *Phys. Rev. Letters* **1**, 199 (1958); *J. Phys. Chem. Solids* (to be published).

spectra, arising from the precipitate, attributed to silica ( $\text{SiO}_2$ ), have been reported.<sup>11</sup> The rate of precipitation depends upon the presence of nucleation centers.<sup>6,12</sup>

(12) Heat-treatment at 1000°C "stabilizes" silicon crystals in that the formation of donors is greatly reduced in the subsequent heat treatment at 450°C.<sup>1,2</sup> No extensive donor activity is present after heating at 1000°C.<sup>1,6</sup>

(13) The spectroscopy of the excited states of the donors produced at 430°C indicates the presence of a multiplicity of oxygen-containing donors whose symmetries are less than tetrahedral.<sup>10</sup>

(14) Several trapping levels have been found in silicon which have been shown to be associated with the formation of donors during heat treatment at 460°C.<sup>13,14</sup> The kinetics of the  $\beta$  trap (capture cross section  $8 \times 10^{-18}$  cm<sup>2</sup>, trapping level 0.71 eV above the valence band, decay constant about 100 sec) were investigated in more detail.<sup>15</sup> It shows the following features: (a) more rapid appearance than the major donors (considerable concentrations have been found in "as grown" crystals), (b) during heat treatment proceeding at 460°C the trap concentration assumes a value much smaller than the maximum donor concentration, (c) rapid reduction of trap density during heating at higher temperatures (e.g., at 700°C the trap density could be reduced from  $1 \times 10^{14}$  to  $3 \times 10^{11}$  cm<sup>-3</sup> within 5 sec).

### C. MECHANISM FOR HEAT TREATMENT

The model which explains all of the kinetic observations discussed in the previous section is based on the following three major assumptions:

(1) The formation of silica ( $\text{SiO}_2$ ), i.e., the polymerization of oxygen observed at high temperatures begins in the course of heat treatment at temperatures as low as several hundred °C.

(2) Certain intermediates in this polymerization are electrically active donors.<sup>16</sup>

(3) Among the intermediate complexes formed those containing more than a certain number of oxygen atoms no longer act effectively as donors at room temperature.

<sup>11</sup> A. Smakula and J. Kalnajs, J. Phys. Chem. Solids (to be published).

<sup>12</sup> S. Lederhandler and J. R. Patel, Phys. Rev. **108**, 239 (1957).

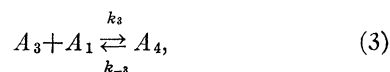
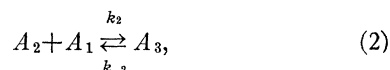
<sup>13</sup> J. A. Hornbeck and J. R. Haynes, Phys. Rev. **97**, 311 (1955); J. R. Haynes and J. A. Hornbeck, Phys. Rev. **100**, 606 (1955).

<sup>14</sup> Hannay, Haynes, and Shulman, Phys. Rev. **96**, 833 (1955).

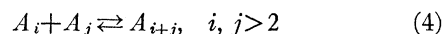
<sup>15</sup> N. B. Hannay and R. G. Shulman (private communication).

<sup>16</sup> The precise manner in which the oxygen is incorporated into the lattice and in particular the physical nature of the donors is not in question here. The authors, in common with other workers in this field, have some notions concerning this matter but the situation remains too uncertain to make positive statements at this time. It should be emphasized that no assumptions concerning the exact nature of the donors (other than the number of oxygen atoms they contain) need be made in order to provide the kinetic analysis of the form presented here.

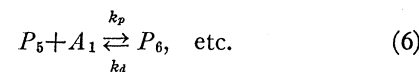
In view of points B4, 9, 10, 13, and 14 of the preceding section and the above assumptions, we associate donor activity in our model with oxygen-containing complexes formed in the initial stages of the aggregation whose final product, silica, can no longer act as a donor at room temperature (B12). Specifically the aggregation begins with oxygen which is initially atomically dispersed and will be denoted by the symbol  $A_1$  (B9,10). We shall use the same symbol to denote the concentration of  $A_1$ , etc. In the course of heat treatment an increasing number of electrically active complexes containing two,  $A_2$ , three,  $A_3$ , four,  $A_4$ , oxygen atoms are built up by the successive reactions:



whose rate constants are indicated. A multiplicity of donor types is in accord with observations B13 and B14. The forward reactions in the crystal characterized by  $k_1$ ,  $k_2$ ,  $k_3$  are probably diffusion limited. At lower temperatures (450°C), the diffusion coefficient of oxygen ( $A_1$ ), while small in magnitude, is still very much larger than that of complexes containing two or more oxygen atoms, so that reactions such as



can be neglected. We assume for reasons which will be evident below that complexes containing more than four atoms of oxygen are no longer appreciably electrically active at room temperature. The aggregation proceeds further according to the sequence of reactions



The  $k_p$  and  $k_d$  will be discussed later. In general, denoting by  $P$  the silica-like polymers formed containing six or more oxygen atoms, the general polymerization and depolymerization reactions can be written symbolically as



In view of the preceding it is reasonable to associate  $A_4$  with a (donor)  $[\text{SiO}_4]$  complex. If this is done some statements concerning the probable relative magnitudes of  $k_1$ ,  $k_{-1}$ ,  $k_2$ ,  $k_{-2}$ ,  $k_3$ , and  $k_{-3}$  can be made. For example,

the known chemical stability of  $[\text{SiO}_4]$  suggests that  $k_{-3} \ll k_3 A_1^0$  or  $k_{-1}$  or  $k_{-2}$ , where  $A_1^0$  is the initial oxygen ( $A_1$ ) concentration. Furthermore, whereas in the forward reactions characterized by  $k_1$  and  $k_2$  the paths by which the involved reactants may combine are fairly numerous, the forward reaction characterized by  $k_3$  requires that the  $A_1$  unit be oriented and placed in precisely the correct position to complete the roughly tetrahedral  $A_4$ . Thus  $k_3$  must have a small steric factor (i.e., small entropy of activation) which in turn suggests that, at around 450°C at least,  $k_3 \ll k_1$  or  $k_2$ .

The preceding inequalities imply that reactions (1) and (2) rapidly approach quasi-equilibrium in comparison with the time required for the equilibration of reaction (3). At certain temperatures, e.g., 450°C, the  $A_4$  must grow progressively at the expense of the (equilibrated)  $A_2$  and  $A_3$  provided only that  $k_3 A_1^0 > k_{-3}$  and  $k_p$  is not prohibitively large. Assuming this to be the case,  $A_4$  will be present in substantially higher concentrations than either  $A_2$  or  $A_3$ , so that most of the observed donor activity is due to  $A_4$ . Under the assumption of equilibrium,

$$A_3/A_1^3 = K_1 K_2, \quad (8)$$

where  $K_1$  and  $K_2$  are the equilibrium constants for reactions (1) and (2):

$$K_1 = k_1/k_{-1}, \quad K_2 = k_2/k_{-2}. \quad (9)$$

Before performing the fairly exact numerical integration of the kinetic equations suggested by our model, we give first an approximate analysis of these equations. This will enable us to compare quickly our simplified model with experimental observations and will provide further insight into the over-all process. We assume tentatively that all depolymerization reactions can be neglected (note that initially we have no polymer) and that  $A_1$  does not differ appreciably from its initial value. Actually the integration of the more exact extended kinetic equations in which depolymerization is included shows that  $A_1(t)$  decreases by less than 20% for  $t < t_{\text{max}}$  (time at which the maximum donor concentration is attained).

Since we are interested in the donor concentration ( $A_4$ ) we apply the law of mass action to (3) and (5), neglecting depolymerization and taking  $A_1 \approx A_1^0$ , to obtain

$$dA_4/dt = k_3 A_1 A_3 - (k_{-3} + k_p A_1) A_4. \quad (10)$$

Substituting (8) in (10), we get

$$dA_4/dt = k_3 K_1 K_2 A_1^4 - (k_{-3} + k_p A_1) A_4. \quad (11)$$

Equation (11) shows that as long as we assume quasi-equilibrium for species  $A_2$  and  $A_3$  we can introduce an effective reaction



where

$$k_f = k_3 K_1 K_2$$

is an effective forward rate constant and  $k_{-3} = k_b$ .

The equation

$$dA_4/dt = k_f A_1^4 - (k_b + k_p A_1) A_4 \quad (12a)$$

can account for a considerable amount of the heat-treatment phenomena discussed in Sec. B.

#### D. COMPARISON BETWEEN THE SIMPLE MODEL AND EXPERIMENTAL OBSERVATIONS

The most extensive experimental data were obtained at an annealing temperature of 450°C. They will be analyzed first.

Since  $A_4$  is initially present in zero concentration, (12a) reduces to

$$(dA_4/dt)_{t=0} = k_f A_1^4, \quad (13)$$

in accord with observation B5. From (13) and Fig. 3 the value of  $k_f$  can be found, e.g., at 450°C,

$$k_f = 1.2 \times 10^{-60} \text{ cm}^9 \text{ sec}^{-1}. \quad (14)$$

Setting the right side of (12a) equal to zero, we obtain  $A_4^*$ , the maximum  $A_4$  concentration, in terms of  $A_1^0$  ( $\approx A_1$ ),

$$A_4^* = \frac{k_f A_1^4}{k_b + k_p A_1} \approx \frac{k_f (A_1^0)^4}{k_b + k_p A_1^0}, \quad (15)$$

which shows that  $A_4^*$  varies directly with the third or fourth power of  $A_1^0$  according as  $k_b \ll k_p A_1^0$  or  $k_b \gg k_p A_1^0$ . As discussed above we expect that  $k_b$  is quite small and hence conclude that at least in first approximation

$$A_4^* \approx (k_f/k_p) (A_1^0)^3, \quad (16)$$

in accord with observation B6. From (16) and Fig. 4 we can find  $k_f/k_p$ , e.g., at 450°C,

$$k_f/k_p = 5 \times 10^{-38} \text{ cm}^6. \quad (17)$$

Substituting (15) in (12a), we find

$$dA_4/dt = (k_b + k_p A_1) (A_4^* - A_4) = \kappa (A_4^* - A_4). \quad (18)$$

This linear equation can be integrated directly (keeping in mind that  $A_1$  is considered to be constant) under the initial condition  $A_4(t=0) = 0$  to give

$$\ln[A_4^* - A_4(t)] = \ln A_4^* - \kappa t, \quad (19)$$

which accords with the observed kinetic behavior discussed under B1. From the slope of the line of Fig. 2 we find that at 450°C

$$\kappa = k_b + k_p A_1 = 1.8 \times 10^{-5} \text{ sec}^{-1}. \quad (20)$$

Neglecting  $k_b$  in comparison with  $k_p A_1$  and choosing  $A_1 \approx 10^{18} \text{ cm}^{-3}$ , we find that

$$k_p = 1.8 \times 10^{-23} \text{ sec}^{-1} \text{ cm}^3. \quad (21)$$

We now have available from three different sources

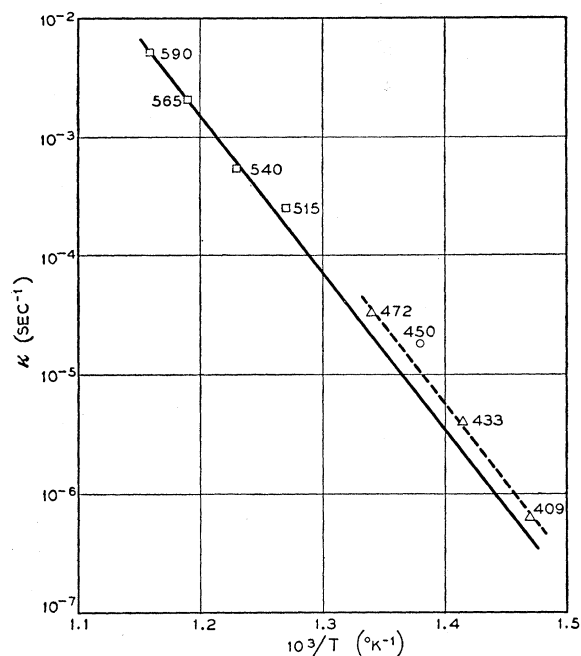


FIG. 5. Experimentally determined reaction constant  $\kappa \approx k_p A_1$  plotted as a function of temperature. Different symbols represent different crystals.

enough data to check the internal consistency of the theory. Thus (17) should be obtained when (14) is divided by (21). The result of the division is

$$k_f/k_p = 7 \times 10^{-38} \text{ cm}^6, \quad (22)$$

which compares favorably with (17).

Next we consider the decay, at temperatures exceeding 500°C, of  $A_4$  generated previously by heat treatment at a lower temperature. Figure 9 of reference 2 exhibits the typical time dependence of this decay. It appears as though the logarithm of the donor concentration remaining after a time  $t$  depends linearly on  $t$ . This behavior we exhibit directly by integrating (18) under the new initial condition  $A_4(t=0) = A_4^0$ , where  $A_4^0$  represents the donor concentration formed after heat treatment at the lower temperature. We find

$$A_4(t) = A_4^*(1 - e^{-\kappa t}) + A_4^0 e^{-\kappa t}. \quad (23)$$

Since  $A_4^0$  is generally of the order of the maximum donor concentration attained at the lower temperature and since it is an experimental fact that the maximum donor concentration decreases rapidly with increasing temperature, we expect that

$$A_4^*(\text{at the higher temperature}) \ll A_4^0,$$

so that (23) reduces to the observed relation (see B2)

$$A_4(t) \sim A_4^0 e^{-\kappa t}. \quad (24)$$

Using (24),  $\kappa$  can be determined at 510°C, 540°C, 565°C, and 590°C from Fig. 9 of reference 2. The values of the

logarithm of  $\kappa$ , so determined, are plotted in Fig. 5 as a function of the reciprocal absolute temperature. The activation energy of  $\kappa$  is found to be 2.8 ev.

Finally we compare the experimental observations for heat-treatment temperatures below 450°C with the kinetics developed above. It will be shown that the data available at this temperature range are consistent with the information obtained at 450°C and higher.

For  $T < 500^\circ\text{C}$  the rate of donor formation decreases and the maximum donor concentration increases with decreasing temperature. These facts can be seen in Fig. 6.<sup>17</sup> At 409°C and below, the donor maximum is not attained even after 520 hours of treatment.

The data obtained during a heat treatment at 472°C can be readily analyzed for  $t < t_{\text{max}}$  in the way discussed in B1 (see Fig. 2). The  $\kappa$  value obtained is in good agreement with other values discussed above (see Fig. 5).

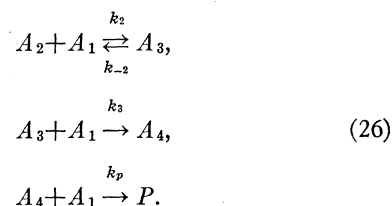
The measurements at 433°C and 409°C exhibit an interesting new feature. At 433°C a maximum of added donors is reached after several hundreds of hours of heat-treatment. For reasons which will be apparent below we shall denote the concentration of added donors by  $A$  rather than by  $A_4$  as previously. If, at 433°C,  $\ln(A^* - A)$  is plotted *versus* time (see Fig. 2), the data fall on an excellent straight line for times exceeding 5 hours. Below this time, however, the curve bends up from the straight line so that the intercept at time zero lies above the intercept obtained by extrapolation of the long-time straight line.

As we shall show below, this result is compatible with the assumption that at lower temperatures (e.g., at 433°C and below) other donors besides  $A_4$  need to be considered. These might be either species  $A_2$  or  $A_3$  or both which may exhibit donor properties and whose quasi-equilibrium concentrations are increased relative to  $A_4^*$  as the temperature is lowered. The rate of achievement of quasi-equilibrium for  $A_2$  and  $A_3$  may be sufficiently reduced at low temperature so that now the contribution to the over-all kinetics of these species may have to be considered specifically on the time scale of the experiment.

To simplify matters, assume that  $A_2$  still achieves quasi-equilibrium very rapidly so that we can write

$$A_2/A_1^2 = K_1, \quad (25)$$

but that the kinetics of the formation of  $A_3$  and  $A_4$  must be considered in detail:



<sup>17</sup> From Fig. 7 of reference 2 and unpublished data by C. S. Fuller.

We assume that  $k_b = k_d = 0$  and that  $A_1$  remains constant as in our previous simple analysis. It can be shown that the dependences of  $A_3$  and  $A_4$  on time are the following:

$$A_3 = k_2 K_1 A_1^3 \left\{ \frac{1}{\kappa_3} (1 - e^{-\kappa_3 t}) \right\}, \quad (27)$$

$$A_4 = \frac{k_2 k_3 K_1 A_1^4}{\kappa_3 - \kappa_4} \left\{ \frac{1}{\kappa_4} (1 - e^{-\kappa_4 t}) - \frac{1}{\kappa_3} (1 - e^{-\kappa_3 t}) \right\}, \quad (28)$$

where

$$\kappa_3 = k_3 A_1 + k_{-2}, \quad \kappa_4 = k_p A_1, \quad (29)$$

so that if  $A$  is the sum of  $A_3$  and  $A_4$ , then

$$\begin{aligned} A &= \frac{k_2 K_1 A_1^3}{\kappa_3} \left[ 1 - \frac{k_3 A_1}{\kappa_3 - \kappa_4} \right] (1 - e^{-\kappa_3 t}) + \frac{k_2 k_3 K_1 A_1^4}{\kappa_4 (\kappa_3 - \kappa_4)} (1 - e^{-\kappa_4 t}) \\ &= C_3 (1 - e^{-\kappa_3 t}) + C_4 (1 - e^{-\kappa_4 t}). \end{aligned} \quad (30)$$

From (30) it follows that  $A^* = C_3 + C_4$  so that

$$A^* - A = C_3 e^{-\kappa_3 t} + C_4 e^{-\kappa_4 t}. \quad (31)$$

If, as we have been assuming all along,

$$\kappa_3 \gg \kappa_4, \quad (32)$$

(so that  $A_2$  and  $A_3$  reach quasi-equilibrium) then (31) shows that at long times

$$A^* - A \approx C_4 e^{-\kappa_4 t}, \quad (33)$$

so that  $\ln(A^* - A)$  is indeed a linear function of time. On the other hand, at earlier times the term  $C_3 e^{-\kappa_3 t}$  must be included, which raises  $A^* - A$  above the extrapolation of the straight line as is observed in Fig. 2.

There are a few independent sources of information which are consistent with this picture. First, it has been observed by Hrostowski<sup>10</sup> that heat treatment gives rise to more than one species of donor. This conclusion is based on a spectroscopic study of the excited states of the donors introduced by heat-treatment. Second, the appearance of traps (B14) during heat treatment suggests that these are  $A_2$  or  $A_3$  since they come to equilibrium very rapidly and at a concentration much less than  $A_4^*$ . They also disappear rapidly at high temperatures, a behavior to be expected, for example, on the basis of the kinetics leading to Eq. (30).

For the measurement at 409°C a donor maximum  $A^*$  is not available. We chose a value of  $A^* = 3.5 \times 10^{16} \text{ cm}^{-3}$  in order to obtain a good fit of the experimental points to a straight line for  $t > 100$  hours in Fig. 2.  $C_4$  can be estimated from the intercept with the ordinate and  $\kappa_4$  is obtained from the slope.

In Fig. 5 the values for  $\kappa$ , obtained between 590°C and 409°C, are summarized. The good agreement of all points with a common line of activation energy 2.8 eV strongly supports the assumption made above that the formation and destruction of donors is affected by the same reaction constant  $\kappa$  which is essentially  $k_p$ ,

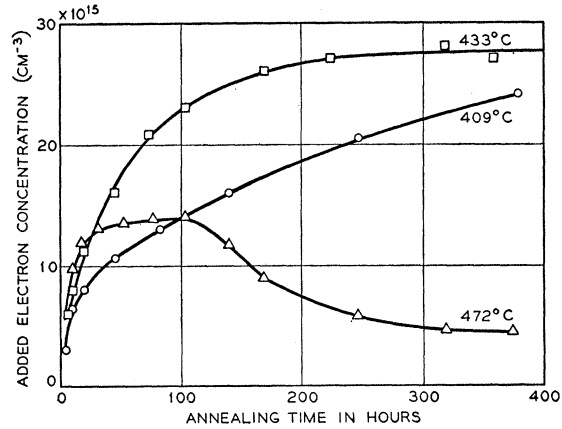


FIG. 6. Added electron concentration versus annealing time for temperatures below 500°C.

the polymerization constant. It should be pointed out that  $\kappa = k_b + k_p A_1$  is a function of  $A_1$ . Variation in the oxygen concentration of the various samples can easily account for the shift of the two sets of data in Fig. 5.

#### E. INTEGRATION OF THE KINETIC EQUATIONS OF THE MORE EXTENDED MODEL

In order to study certain features of our model, particularly its behavior at longer times, we can no longer neglect the depolymerization reactions or assume that  $A_1$  remains constant. Clearly we can in sufficient approximation treat the formation and dissociation of  $A_2$  and  $A_3$  by the quasi-equilibrium as before.

Applying the principle of mass action to Eqs. (5) to (7), etc., we obtain the nonlinear system

$$\begin{aligned} dA_1/dt &= 4k_b A_4 + k_d [P_5 + P] - 4k_f A_1^4 \\ &\quad - k_p A_1 [A_4 + P_5 + P], \end{aligned} \quad (34)$$

$$dA_4/dt = k_f A_1^4 + k_d P_5 - k_b A_4 - k_p A_1 A_4, \quad (35)$$

$$dP_5/dt = k_p A_1 A_4 + k_d P_5 - k_a P_5 - k_p A_1 P_5, \quad (36)$$

etc. We set, as before,  $P = \sum_{n=6} P_n$ . Since we are primarily interested in the behavior of  $A_1$  and the principal donor species  $A_4$ , we close the system of equations by assuming that in first approximation

$$k_d P_5 \approx k_a P_5. \quad (37)$$

This condition is reasonable in view of the possibility that  $k_d$  itself may vary slightly with the number of oxygen atoms and the fact that  $k_d$  is fairly small in comparison with  $k_p A_1^0$ . Equation (36) thus reduces to

$$dP_5/dt \approx k_p A_1 A_4 - k_p A_1 P_5. \quad (38)$$

Finally the change in time of  $P$  is given by the total flux of material passing from  $P_5$  to  $P_6$ , i.e.,

$$dP/dt = (k_p A_1 P_5 - k_a P_5) \approx (k_p A_1 - k_a) P_5. \quad (39)$$

This nonlinear system describes the evolution of heat

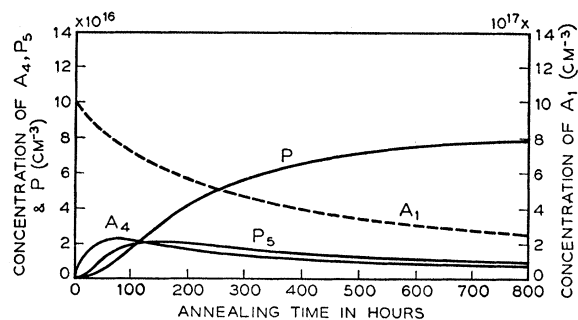


FIG. 7. Calculated change with annealing time of the oxygen concentration  $A_1$ , the  $[\text{SiO}_4]$  complexes  $A_4$ , and the polymers  $P_5$  and  $P$ . Annealing temperature  $450^\circ\text{C}$ . Initial oxygen concentration  $A_1^0 = 10^{18}$  atoms  $\text{cm}^{-3}$ .

treatment when integrated under the initial conditions

$$A_1(0) = A_1^0, \quad A_4(0) = 0, \quad P_5(0) = 0, \quad P(0) = 0. \quad (40)$$

This integration can be accomplished most expeditiously by using the multiple-purpose electrical analog computer<sup>18</sup> (we require an accuracy of only a few percent).

After introducing a suitable scaling transformation, Eqs. (34), (35), (38), and (39) were integrated and the output ( $A_1$ ,  $A_4$ ,  $P_5$ ,  $P$ ) of the computer was directly recorded on graph paper. The initial value of  $A_1$  [see (40)] was estimated from the experiment. The rate constants  $k_f$ ,  $k_p$ ,  $k_d$  were adjusted to obtain a good fit of the experimental data at  $450^\circ\text{C}$ . The values of  $k_f$  and  $k_p$  correspond quite well with those obtained from the more elementary analysis of the previous section.  $k_d$  could be crudely estimated from heat-treatment data. Good agreement between experimental data and the calculated curve  $A_4$  was obtained for negligible values of  $k_b$  ( $< 10^{-8}$   $\text{sec}^{-1}$ ). This small value of  $k_b$  was expected from our earlier discussion.

A number of the more interesting graphs obtained in this way by varying  $A_1^0$  (at constant temperature) and/or the rate constants (corresponding to temperature changes) are shown in Figs. 7 to 10. These graphs reproduce quite vividly most of the kinetic observations

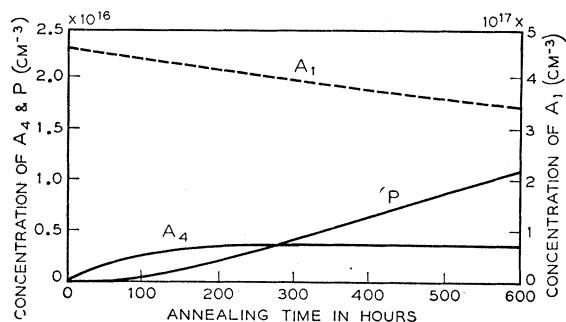


FIG. 8. The same calculation as Fig. 7 with  $A_1^0 = 0.45 \times 10^{18}$   $\text{cm}^{-3}$ .

<sup>18</sup> A. A. Currie and E. Lakatos, Bell Labs. Record 29, No. 3, 3 (1951).

of Sec. B and justify the elementary analysis of the preceding section.

Consider Fig. 7 which corresponds to the heat treatment at  $450^\circ\text{C}$  of a silicon crystal containing initially  $10^{18}$  atoms of oxygen per  $\text{cm}^3$ . The rate constants,  $k_p = 7.7 \times 10^{-24}$  ( $\text{cm}^3 \text{sec}^{-1}$ ),  $k_f = 3.1 \times 10^{-61}$  ( $\text{cm}^3 \text{sec}^{-1}$ ),  $k_d = 1.3 \times 10^{-6}$  ( $\text{sec}^{-1}$ ), and  $k_b = 0$  correspond quite well with those expected [see Eqs. (14) and (21)]. We note: (1) The rapid rise of  $A_4$  to the maximum whose shape, height, and location (in time) is in excellent agreement with experiment as can be seen from Fig. 1. (2) At the time at which  $A_4$  reaches a maximum,  $t_{\text{max}}$ ,  $A_1$  has fallen only to 80% of  $A_1^0$ , which justifies the neglect of the variation of  $A_1$  in the previous section. (3) The maximum in  $P_5$  and the region of extended rise in  $P$  occur after  $t_{\text{max}}$ , justifying in first approximation the neglect of depolymerization reactions in the simplified kinetics.

The effect of reducing  $A_1^0$  to  $0.45 \times 10^{18}$  atoms/ $\text{cm}^3$  is shown in Fig. 8, which corresponds again to heat treatment at  $450^\circ\text{C}$ . We note particularly (1) the smaller rate of formation of  $A_4$ , the smaller height of the  $A_4$  maximum which is attained after a considerably longer time (several hundred hours), and (2) the very small decrease of  $A_1$  with time.

The effect on heat treatment at  $450^\circ\text{C}$  of increasing  $A_1$  to  $1.8 \times 10^{18}$  atoms/ $\text{cm}^3$  is shown in Fig. 9. The rapid rise and decay of  $A_4$  as well as the height of the maximum accord well with experimental observations.<sup>8</sup>  $A_1$  decreases quite rapidly for  $t < t_{\text{max}}$ .

It is quite apparent from Figs. 7 to 9 that small changes (factor of 4) of oxygen concentration in silicon has a very strong effect on the formation of donor states. As pointed out in B8, silicon crystals pulled without rotation exhibit a considerably smaller donor formation after heat treatment at  $450^\circ\text{C}$ . It is believed that the small oxygen content of these crystals is the major cause for this effect. Silicon crystals of defined, larger oxygen contents were prepared without rotation in a floating-zone system by adding a controlled partial pressure of oxygen or water to the gaseous ambient medium. These crystals showed the same heat-treatment effects as pulled, rotated ingots of comparable oxygen content (see Fig. 4).

The effect of lowering the temperature of the heat treatment to  $430^\circ\text{C}$  is shown in Fig. 10.  $A_1^0$  is again  $10^{18}$  oxygen atoms/ $\text{cm}^3$ . The rate constants are  $k_f = 1.1 \times 10^{-61}$  ( $\text{cm}^3 \text{sec}^{-1}$ ),  $k_p = 1.3 \times 10^{-24}$  ( $\text{cm}^3 \text{sec}^{-1}$ ),  $k_d = 2.2 \times 10^{-7}$  ( $\text{sec}^{-1}$ ), and  $k_b = 0$ . We note in accord with experimental observation (1) that  $A_4$  is formed at a considerably smaller rate, (2) an increase of  $A_4^*$  which is attained only after several hundred hours of heating, and (3) the fact that considerably fewer polymers are formed.

As discussed in B12, annealing at  $1000^\circ\text{C}$  does not provide an appreciable donor concentration and also reduces the rate and maximum number of donors in a subsequent heat treatment at  $450^\circ\text{C}$ . It was shown above

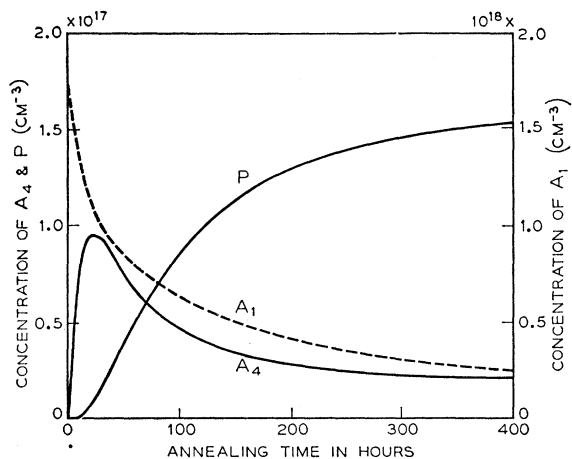


FIG. 9. Calculated curves for  $A_1$ ,  $A_4$ , and  $P$  using the same parameter as in Fig. 8. Initial oxygen concentration  $A_1^0 = 1.8 \times 10^{18}$  atoms  $\text{cm}^{-3}$ .

that polymers of various size are being formed at high temperatures. Their subsequent slow depolymerization at  $450^\circ\text{C}$  (together with the oxygen content still in solid solution) gives rise to the formation of (donors)  $A_4$ . As an example, we have integrated Eqs. (34), (35), (38), and (39) using the initial conditions

$$A_1^0 = 2 \times 10^{17}, \quad A_4(0) = 0, \quad P_5(0) = 10^{16}, \quad P(0) = 0,$$

and the rate constants listed above for the  $450^\circ\text{C}$  annealing. It could be shown that donors ( $A_4$ ) up to a concentration of  $3 \times 10^{15}/\text{cm}^3$  are formed after several hundred hours of annealing.

#### F. DISCUSSION

Since the polymerization reaction is probably diffusion controlled,  $k_p$  should have the form<sup>19</sup>

$$k_p = 4\pi RD, \quad (41)$$

where  $D$  is the diffusion coefficient of  $A_1$  and  $R$  is an effective capture radius for  $A_1$ . Assuming short-range

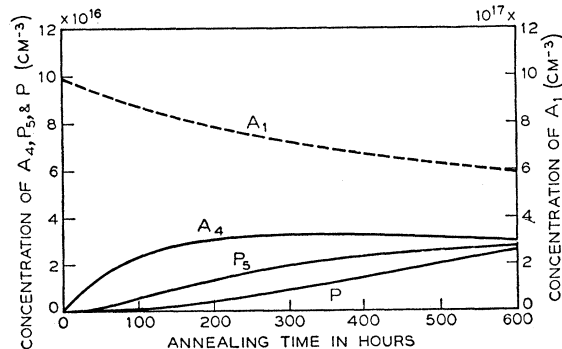


FIG. 10. Calculated change of  $A_1$ ,  $A_4$ ,  $P_5$ , and  $P$  versus annealing time for a temperature of about  $430^\circ\text{C}$ . Initial oxygen concentration  $A_1^0 = 10^{18}$  atoms  $\text{cm}^{-3}$ .

<sup>19</sup> T. R. Waite, J. Chem. Phys. 28, 103 (1958).

forces,  $R$  may be approximated by an average geometrical radius of the polymer. If the reaction is truly diffusion limited, then the activation energy of  $R$  should be small compared to that of  $D$  and the activation energy for  $k_p$  should therefore be essentially that of  $D$ .<sup>19</sup>

The most reliable information on the activation energy for the diffusion coefficient of oxygen in silicon seems to be that obtained from strain-aging studies performed by Pearson, Read, and Feldman.<sup>20</sup> They quote the value 3.1 eV which compares favorably with the 2.8 eV found above for  $k_p$ .

By using (41),  $D$  can be computed from a measured value of  $k_p$  if  $R$  is estimated. We shall choose  $R = 5 \times 10^{-8}$  cm. This estimate is probably correct within a factor of 2 and the same error thus applies to the value of  $D$  derived below. For  $k_p = 7.7 \times 10^{-24}$   $\text{cm}^3 \text{sec}^{-1}$ , the value used in connection with Figs. 7, 8, and 9, we obtain

$$D = 3 \times 10^{-18} \text{ cm}^2/\text{sec}. \quad (42)$$

Estimates using a combination of Logan's<sup>7,8</sup> data and those of Pearson *et al.*<sup>20</sup> on the diffusion of oxygen in silicon lead one to expect a value near  $10^{-20}$   $\text{cm}^2/\text{sec}$  at  $450^\circ\text{C}$ . However, owing to the uncertainty in the original data and the length of the extrapolation from high to low temperatures, the error could easily be several orders of magnitude.

Another question requiring discussion is the role of nucleation in our scheme. In the models presented, no mention has been made of nucleation and indeed the phenomenon is not contained implicitly in the equations we have set forth. Nevertheless point B11 indicates that some attention must be given to the matter.

Until now we have been careful to use the word *aggregate* rather than *precipitate* because we do not wish to have the small complexes whose concentrations are dealt with by the above equations regarded as precipitates. They are still part of the original phase, being in fact solutes. As these aggregates continue to grow, both  $k_p$  and  $k_d$  must show some dependence on size. In fact, Eq. (41) for  $k_p$  demonstrates that the latter depends on  $R$  and therefore roughly on the cube root of the number of oxygen atoms contained in the polymer. This dependence is sufficiently small so that over a small range of sizes  $k_p$  may be considered constant.

The constant  $k_d$  also has a size dependence which has been neglected in our previous considerations. This size dependence is related among other things to the work required to form an interface between the polymer (when large enough to be treated as an embryo of a new phase) and the surrounding silicon. In fact, if we adopt the standard considerations of nucleation theory,<sup>21</sup> the net rate at which a polymer of size  $n$

<sup>20</sup> Pearson, Read, and Feldmann, Acta Met. 5, 181 (1957), and private communication.

<sup>21</sup> J. Frenkel, Kinetic Theory of Liquids (Oxford University Press, Oxford, 1946), Chap. 8; H. Reiss, Z. Elektrochem. 56, 459 (1952).



becomes one of size  $n+1$  passes through a severe minimum at some size  $n^*$ . This minimum is directly related to the size variations of  $k_p$  and  $k_d$  and occurs at that polymer which is fashioned from monomers with the maximum expenditure of free energy. This polymer of size  $n^*$  is commonly called the nucleus.

The existence of the rate minimum described above results in a severe bottleneck in the flow of polymer through the various sizes and may become severe enough so that the size  $n^*$  is to all intents and purposes impassable. Under these conditions, which probably exist at a low temperature such as 450°C, equilibrium is attained among aggregates smaller than size  $n^*$  but not beyond. As a result the collapse of supersaturation is prevented and a constrained equilibrium in which the large true value of  $A_1$  may be very high is reached. This explains why the value of  $A_1$  after a long time (when equilibrium has apparently been reached) in Fig. 7 is much higher than extrapolations of high-temperature measurements<sup>10</sup> on oxygen solubility. For example, in Fig. 7 it appears to be  $10^{17}$  cm<sup>-3</sup> while on the basis of extrapolation one might expect  $10^{14}$  cm<sup>-3</sup>.

At higher temperatures the rate constants are sufficiently large so that the barrier at  $n^*$  can be pierced during experimentally realizable intervals of time and the true solubility can be measured. Under these conditions one must expect that the existence of nucleation centers of various kinds influences the overall kinetics, and of course there is evidence for this (see B11). On the other hand at 450°C, we are probably safe in ignoring phenomena associated with nucleation and this is the assumption made in the formulation of the equations used.

When comparison is made between experimental observations and the model outlined above three important facts should be kept in mind.

(1) Recent experimental work indicates a direct interaction between oxygen and a number of chemical impurities. In particular the formation of complexes

between oxygen and Al,<sup>22</sup> Ga,<sup>22,23</sup> B,<sup>22</sup> and Li<sup>24</sup> has been inferred from electrical, optical, and precipitation studies. High-resistivity silicon specimens are frequently compensated with respect to donor and acceptor impurities. Their presence will obscure the kinetics discussed here, since our model is concerned with the interaction of oxygen and silicon only.

(2) Infrared investigations showed that the oxygen concentration in silicon ingots can vary strongly parallel and perpendicular to the pulling axis of the crystal.<sup>5,6</sup> In addition small-scale fluctuation of oxygen coinciding with the growth-ring patterns of the crystal have been observed.<sup>6,25</sup> Because of the strong dependence of the donor formation upon the oxygen concentration only specimens with uniform oxygen distribution are useful for quantitative investigations.

(3) During the normal cooling process silicon crystals experience a heat treatment depending upon a number of crystal growing parameters. As a result, "as grown" silicon crystals contain varying amounts of thermal donors<sup>6</sup> and traps.<sup>13,14</sup> In order to have oxygen in an initially dispersed state and to destroy small oxygen aggregates, already formed, a short heating of the specimen to high temperatures ( $T \gtrsim 1200^\circ\text{C}$  depending upon the oxygen concentration to be dissolved) proved to be sufficient to "normalize" the sample.<sup>26,27</sup>

#### ACKNOWLEDGMENTS

The authors are greatly indebted to C. S. Fuller, H. J. Hrostowski, R. A. Logan, and R. G. Shulman for communication and discussion of unpublished experimental work. Valuable comments by N. B. Hannay and C. D. Thurmond are greatly appreciated.

<sup>22</sup> C. S. Fuller and F. H. Doleiden, *J. Appl. Phys.* **29**, 165 (1958).

<sup>23</sup> H. J. Hrostowski and R. H. Kaiser, *J. Phys. Chem. Solids* **4**, 148 (1958).

<sup>24</sup> E. M. Pell, presented at Brussels Conference, 1958.

<sup>25</sup> W. C. Dash (to be published).

<sup>26</sup> C. S. Fuller (private communication).

<sup>27</sup> N. B. Hannay and R. G. Shulman found that a trap density ( $\beta$  trap) of  $5 \times 10^{13}$  cm<sup>-3</sup> decreased below the limit of detectability of  $3 \times 10^{10}$  cm<sup>-3</sup> within 30 sec at 1400°C.